Chapter-5

Extremely Low-frequency Magnetic Field Exposure Induced Antiproliferative Activity Against Selective Cancer Cells: An *In- Vitro* Study

5.1 Introduction

The effects of ELF-MF< 100 kHz on biological system has been the subject of scientific interest as well as public debate for decades (Ahlbom et al., 2008; Belyaev et al., 2016). Therefore, various investigations conducted primarily focused on possible ELF-MF exposure effects on growth regulatory genes (Funk et al., 2009; Thrivikraman et al., 2018), cellular signalling (Mahna et al., 2014; Spyridopoulou et al., 2018), receptor-mediated signal transduction (Barati et al., 2021; Uckun et al., 1995), calcium signalling (Ghodbane et al., 2013; Panagopoulos et al., 2002), and in recent cases, anti-neoplastic potential is also observed (Crocetti et al., 2013; Filipovic et al., 2014). According to the aforementioned research, MFs clearly affect cellular and molecular mechanisms. Specifically, these alterations could lead to significant alterations in cell morphologies and proliferation. In humans and animals, the so-called "promotional" phase of carcinogenesis, mutant cells have a growth advantage over non-mutated cells due in large part to unchecked cell proliferation (Foster, 1997).

Although there have been various investigations of possible biological effects of ELF-PEMF on cell proliferation and morphologies, but the results have been largely inconsistent (Hall et al., 2005; Radeva and Berg, 2004). The objective of this study is to provide a proof of concept of how a Helmholtz coil system, described in previous studies (Tekam et al., 2023a), can be utilized for screening in a single experiment with three different ELF-MF intensities but identical duration (20 min (twice) with a 4 h gap) to detect any significant changes in cancer cell proliferation, morphology and cytotoxicity.

5.2 Material and methods

5.2.1 Materials

The National Center for Cell Sciences (NCCS), located in Pune, India, provided human breast cancer (MCF-7), hepatoblastoma (HepG2) cells, and lung adenocarcinoma (A549) cells. Dulbecco's modified Eagles medium (DMEM) high glucose, 4',6-diamidino-2-

phenylindole (DAPI) (1:800, Roche, Basel, Switzerland), 3-(4,5-Dimethylthiazol-2-yl)-2,5-diphenyltetrazolium bromide (MTT), fetal bovine serum (FBS), phosphate-buffered saline (PBS), paraformaldehyde, bovine serum albumin (BSA), trypan blue, trypsin, glycerol, ethylenediaminetetraacetic acid (EDTA), dimethyl sulfoxide (DMSO, HiMedia), rhodamine-phalloidin (1:150, Invitrogen, Carlsbad, CA, USA), triton X 100, penicillin and streptomycin solution (100X) were purchased from HiMedia, India. Distilled water and absolute ethanol (99.9%) were used in every experiment.

5.2.2 50 Hz ELF-PEMF exposure system

The structural design of the custom-made 50 Hz ELF-PEMF exposure system is identical to that provided in our previous publication (Tekam et al., 2023b, 2023a). The design specifications for the cell exposure system are listed in table 5.1. The schema of the horizontal MF exposure system, current characteristics, and photographs of the actual exposure chamber are shown in figure 5.1 (A-F). In the design configuration monoaxial Helmholtz coils were arranged (parallel configuration), and a 0.5 cm thick acrylic sheet exposure chamber (temperature and humidity controlled) is fabricated and placed in the center to ensure homogeneous MF exposure during experimental duration. The generated 50 Hz ELF-PEMFs are horizontally aligned with exposure chamber and effective MF strength of 1-3 mT(rms). The MFs was maintained homogenous inside the exposure chamber (30 cm × 17 cm × 25 cm) with fluctuations within < ± 5%.

Table 5.1 Design specification of 50 Hz ELF-PEMF exposure system

Exposure coil	
Coil type	Mono axial Helmholtz circular coil
Coil outer diameter	
Circular coil-1	0.530 m
Circular coil-2	0.530 m

Coil inner diameter	
Circular coil-1	0.490 m
Circular coil-2	0.490 m
Wire length	
Circular coil-1	898.668
Circular coil-2	898.668
Number of turns	540 (each)
Maximum current	
Circular coil-1	3 A
Circular coil-2	3 A
Maximum magnetic field	3.06 mT
Total resistance	23.3 Ω/coil
Minimum current	
Circular coil-1	1 A
Circular coil-2	1 A
Minimum magnetic field	1.08 mT
Frequency	50 Hz
Exposure chamber	30 cm × 17 cm × 25 cm
Uniformity of field strength	< ± 5% deviation from center
Field direction and polarity	Horizontal, A.C. magnetic field

The fabrication of monoaxial Helmholtz coils with wooden framework has multiple advantages i.e., reduction in eddy current losses, less vibrations and cost effectiveness. We also installed a temperature sensor and controller (tAPMAN 48 7E-1) to maintain temperature (37 ± 2 °C) inside the exposure chamber.

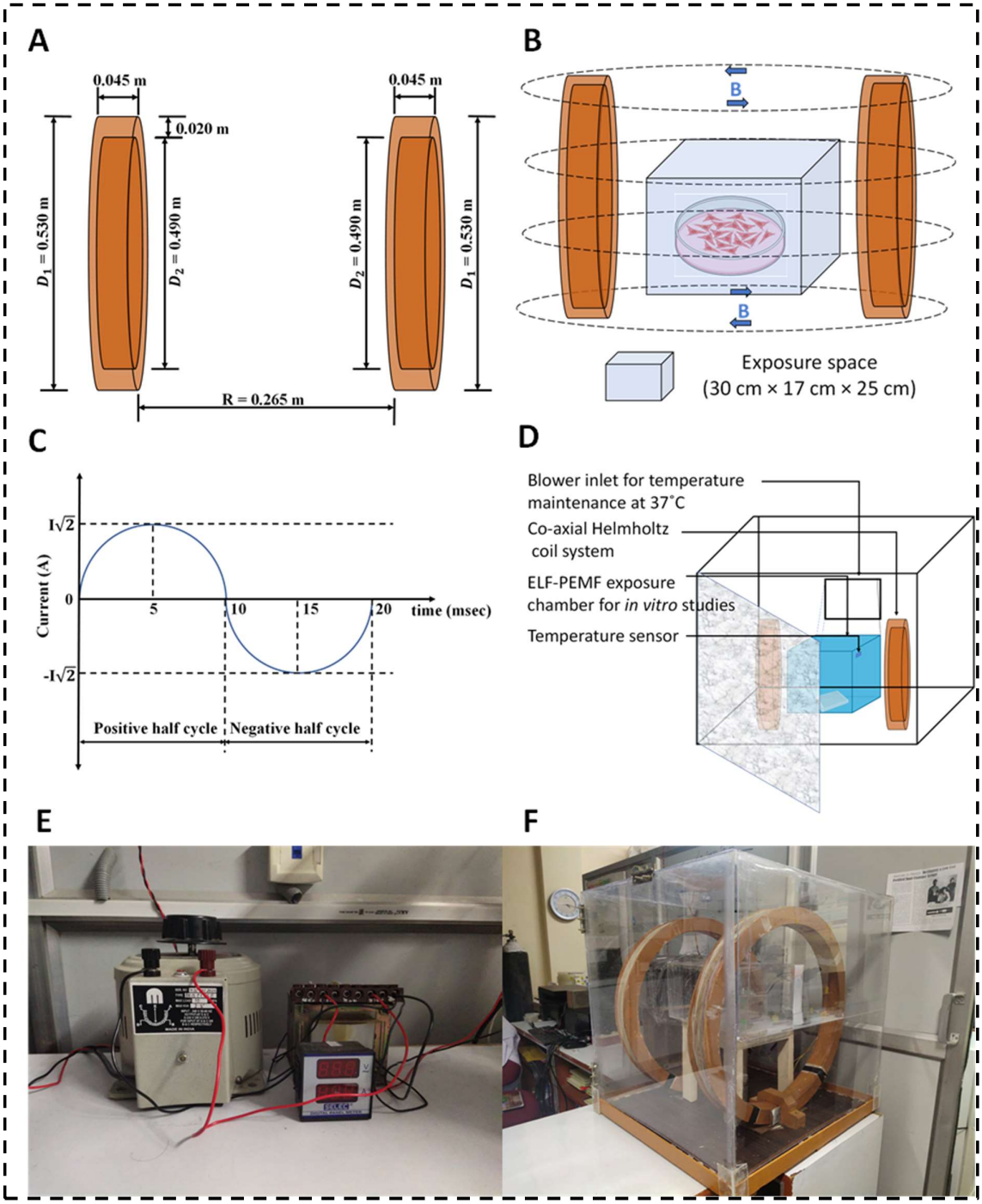

Figure 5.1 50 Hz ELF-PEMF exposure system. **(A)** Schema of horizontal MF generating system, **(B)** Schema for MF exposure (blue arrows indicate the MF direction), **(C)** A.C. current characteristics, **(D)** Schema for MF exposure chamber for *in vitro* analysis (temperature and humidity controlled), **(E)** Arrangement of power supply and digital display monitoring system, **(F)** Prototype of horizontal MF exposure system. Right photograph shows a 2-D alternating MF generating monoaxial coil system. Inner cubic box is an incubation chamber for cell cultivation. Left photograph shows combination of A.C. power supplies, autotransformer and digital ammeter/voltmeter for continuous monitoring.

5.2.3 Cell culture and preparation

The selection of A549, MCF-7, and HepG2 cell lines was made considering the high prevalence of lung, breast, and liver cancers in humans (Mattiuzzi and Lippi, 2019). A549, MCF-7, and HepG2 cells were grown to sub-confluence and released by brief digestion with 0.5% trypsin/0.2% EDTA (trypsin/EDTA). We performed cell counting using the trypan blue method and during process, a mixture of trypan blue (25 µl), culture medium (15 µl), and cells containing medium (10 µl) were utilized.

$$\text{Ratio} = \frac{\text{Total volume}}{\text{cell containing media}} \tag{5.1}$$

$$\text{Calculation formula} = \left(\frac{\text{No.of cells}}{4}\right) \times \text{dilution ratio} \times 10^4 \tag{5.2}$$

The cells were counted into three groups with a manual hemocytometer under the microscope. After harvesting the cells from the culture dishes and rinsing with Ca^{2+} and Mg^{2+} free PBS, 1×10^3 cells/ml suspensions of A549, MCF-7, and HepG2 cells were prepared using DMEM and supplemented with FBS (10%) and antibiotics (1%). We utilized a 96-well culture plate for seeding at a density of 1×10^3 cells per well to encourage cells proliferation. After seeding, the cell culture was kept in an incubator (Galaxy 170S, Eppendorf, Germany) for 24 hours at 37 ± 2˚C, 5% CO2, and 95% humidity to ensure cell adherence and stability.

5.2.4 Experimental protocol

The experimental protocol for *in vitro* studies is shown in figure (5.2). In the current research, cell culture is divided into the following groups: control, 1 mT, 2 mT, 3 mT. The 50 Hz ELF-PEMF exposure was performed with the duration of 20 min (twice) with a 4 h gap at a voltage of $75 \text{ volts} \leq V \leq 190 \text{ volts}$ until the 5th day or confluency (≥ 95%), whichever came first, as depicted in figure (5.2). In our study, the cells in all groups are seeded at density (1×10^3) and during exposure studies the control group attain the confluency (≥ 95%) on day-5 of

experimental duration. The samples were sequentially placed in the ELF-PEMF chamber for stimulation as depicted in figure (5.2) and after exposure transferred back in the incubator (Galaxy 170S, Eppendorf, Germany). The maximum and minimum magnetic flux density used for this study was set at 1 mT and 3 mT, respectively, sufficiently higher than occupational and residential environments. In the current work, we used cancer cell lines from various sources to observe how exposure to an ELF-MF modulate cell proliferation and morphologies. According to literature MFs induce micro-currents in culture dishes to manipulate the electrochemical balance of the cell membrane and, consequently, whole cell function (Dj et al., 2000; Filipovic et al., 2014; Panagopoulos et al., 2002).

The relative humidity in the exposure chamber was maintained by the natural water evaporation in a petri dish but we did not install CO_2 supply unit with the exposure chamber. The primary function of CO_2 supply is to maintain a stable physiological pH in cell culture (Ashdown et al., 2020), and as far as CO_2 supply during MF exposure is concerned, the exposure duration/sample inside the exposure chamber is less than 30 min which is acceptable according to literature (Dubey et al., 2021).

We have utilized bright-field and fluorescent microscopic techniques to observe the cell proliferation and morphologies throughout the experimental duration, as depicted in figure (5.2). In contrast, the cell culture medium was changed every other day. Moreover, cell culture was examined for induced cytotoxicity by a standard microplate absorbance reader (Synergy H1 hybrid, Biotek, USA). Three independent experiments in triplicate were conducted under identical experimental conditions.

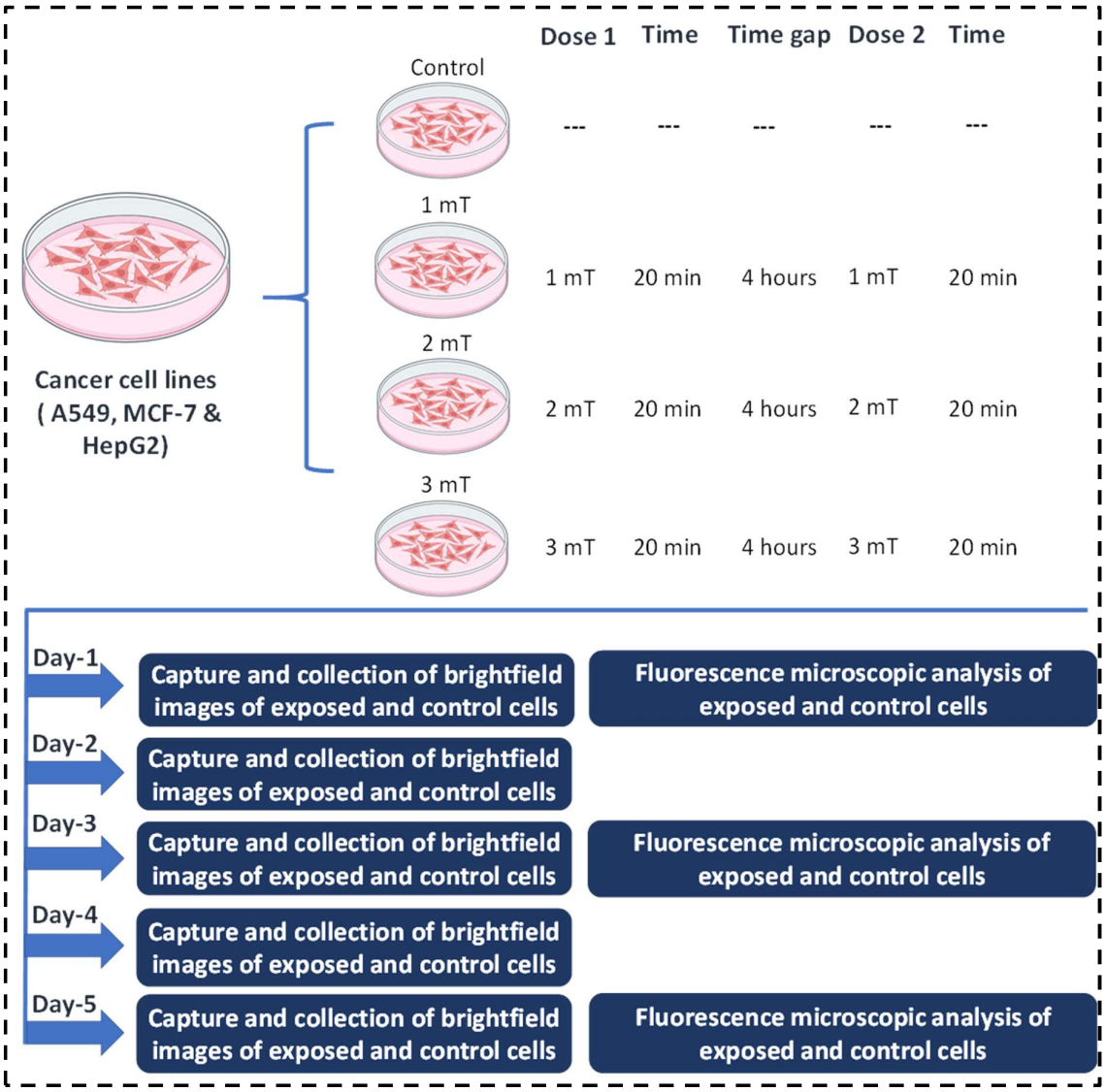

Figure 5.2 Schematic representation experimental protocol for repeated 5-days magnetic field exposure study. In this study, different cancer cell lines were exposed to 50 Hz magnetic field (1-3 mT, 20 min (twice) with 4 h gap) under *in vitro* conditions and observed daily for effect on cell proliferation.

5.2.5 Cell proliferation and morphology analysis

The cell proliferation and morphologies were observed under the microscope (Nikon ECLIPSE Ti-U) to capture bright-field images from day 0 to day 5 of *in vitro* cell culture. Fluorescence can be used in biology as a non-destructive method of analysing biological molecules (Lichtman and Conchello, 2005). In fluorescence microscopy technique, the rhodamine-

phalloidin is utilized for assessment of structural, mechanical, and enzymatic functions of f-actins (Pollard, 2016). DAPI staining is used for the assessment of the changes in cell nuclei in response to therapy or medications (Jablonská et al., 2020). Moreover, the cells were seeded at a density of 1×10^3 on 22 mm coverslips to observe the cell morphology and structure.

The cells were fixed with 4% paraformaldehyde for 15 minutes on days 1, 3, and 5, and cleaned with PBS. The cells were treated with 1 % BSA for 10 min. after being rinsed three times with PBS and permeabilized for 5 min. at temperature (37 ± 2 °C) using Triton X 100 (0.5%). After the PBS wash, rhodamine-phalloidin and DAPI were added to stain actin filaments and cell nuclei, respectively. In the end, we also added glycerol to prevent the cells from drying out. We utilized fluorescent microscope (Nikon ECLIPSE Ti-U) to observe any changes in cell morphology.

5.2.6 MTT assay

Cell viability was evaluated using the MTT reduction assay, as depicted in figure (5.3). In this method the reduction of tetrazolium salt (MTT, yellow colour) to the insoluble formazan is measured for assessment of cytotoxicity (Stockert et al., 2018). The 50 Hz ELF-PEMF exposure protocol was followed as depicted in figure (5.2). After day 1 ELF-PEMF exposure, the culture medium was replaced by a mixture of culture medium (100 µl) and MTT (5 mg/ml in PBS) solutions in a ratio of 10:1. After incubation (4 h), the culture medium was removed, and formazan crystals developed inside the cell culture plates were solubilized using DMSO (100 µl) for 30 min. In the end, the absorbance was measured at wavelength (570 nm) on a multiplate reader (Synergy H1 hybrid, Biotek, USA). We repeated the procedure mentioned above for days 3 and 5, respectively. Each experiment was repeated in triplicate to test the cytotoxicity of exposure to ELF-PEMF intensities.

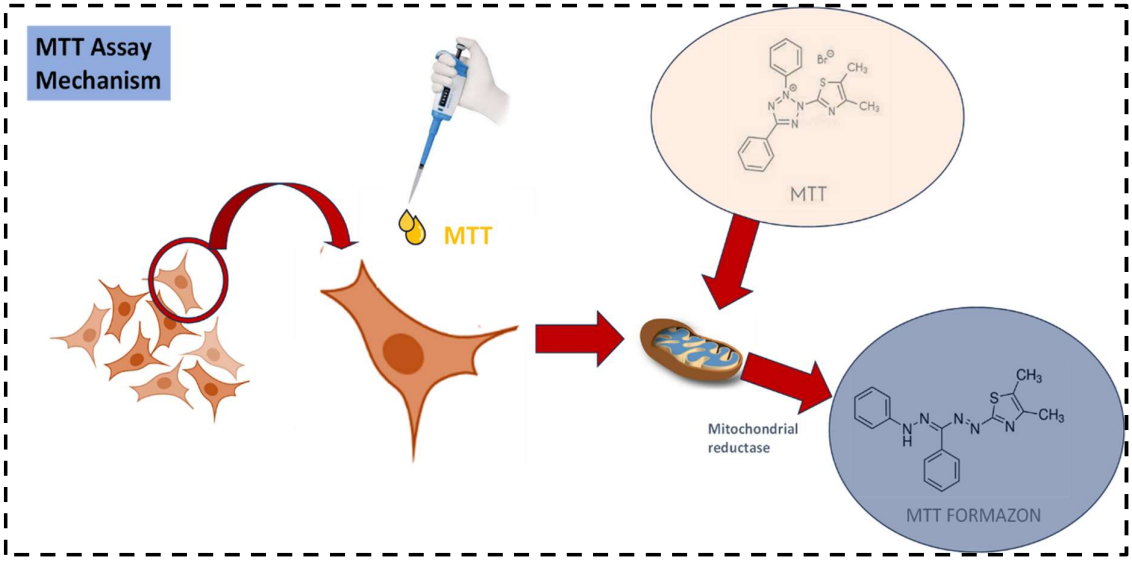

Figure 5.3 Mechanism of MTT assay to determine the cellular proliferation (Stockert et al., 2018).

$$\text{Cell viability}_{\text{test}}(\%) = (\text{Ab}_{\text{test}}/\text{Ab}_{\text{control[5 day]}}) \times 100 \quad (5.3)$$

$$\text{Cell viability}_{\text{control}}(\%) = (\text{Ab}_{\text{control}}/\text{Ab}_{\text{control[5 day]}}) \times 100 \quad (5.4)$$

5.3 Statistical analysis

The experimental data are expressed as mean ± standard deviation (SD) and analyzed by one-way ANOVA followed by Tukey analysis. All statistical analyses were performed on Origin 8.5 (Origin Lab Corporation). ImageJ (Wayne Rasband) was used to remove background noise from brightfield and fluorescent images for better clarity and resolution. The cell culture images are individually corrected using the gaussian blur function, and then the background noise is removed by subtracting the result from the original raw image data. $p < 0.05$ was considered statistically significant.

5.4 Results

5.4.1 Antiproliferative activity

We have observed the difference in cell proliferation among 50 Hz ELF-PEMF exposed and the control group. The cell count % of A549, MCF-7, and HepG2 are shown in figures (5.4-5.6), respectively. The 50 Hz ELF-PEMF inhibited cell count % in A549 cells from day 1 to day 5 compared to control, as shown in figure (5.4).

We also examined the effect of 50 Hz ELF-PEMF exposure on MCF-7 and HepG2 cells apart from A549 cells. The cells were cultured in the identical conditions as A549 cells, and their proliferation was monitored to determine any significant alterations in cell proliferations and morphologies. Figure (5.5) displays a bar plot of cell count % on days 1, 3, and 5 for the MCF-7 in field-exposed and control groups. It reveals that there was no discernible difference in the groups' rates of cell proliferation for the course of the five-day exposure duration. Moreover, figure (5.6) shows a bar plot of cell count % on days 1, 3, and 5 for field exposed and control groups of HepG2 and showed no significant changes in cell proliferation over the entire 5-day growth period between groups.

It's interesting to note that, as figures (5.5–5.6) illustrate, we discovered that there was no discernible change in the percentage of exposed versus control group cells for MCF-7 and HepG2. It reveals that there was no discernible difference in the groups' rates of cell proliferation for the course of the five-day exposure duration.

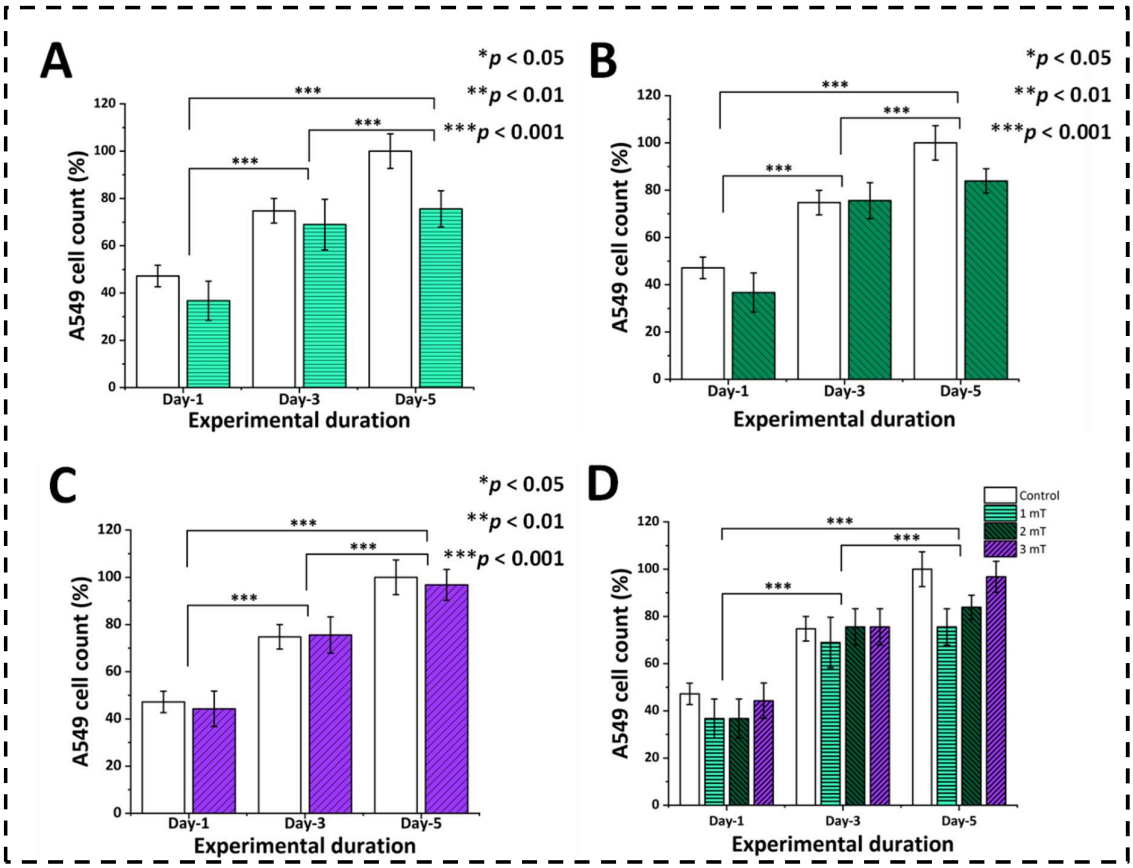

Figure 5.4 Cell count % of adenocarcinoma (A549) cells was significantly affected by the 50 Hz ELF-PEMF exposure (horizontally aligned). A549 cells were counted at different MF intensities (1-3 mT, 20 min (twice) with a 4 h gap) over 5 days. **(A)** Effects of 1 mT on A549 cell count compared to control, **(B)** Effects of 2 mT on A549 cell count compared to control, **(C)** Effects of 3 mT on A549 cell count compared to control, **(D)** Comparative analysis of MF exposure on A549 cells compared to the control group. The initial seeding concentration was 1×10^3 cells/well, and magnetic field exposure till the 5th day or confluency (≥ 95%). The independent exposures were performed in triplicates. "*" $p < 0.05$, "**" $p < 0.01$, "***" $p < 0.001$.

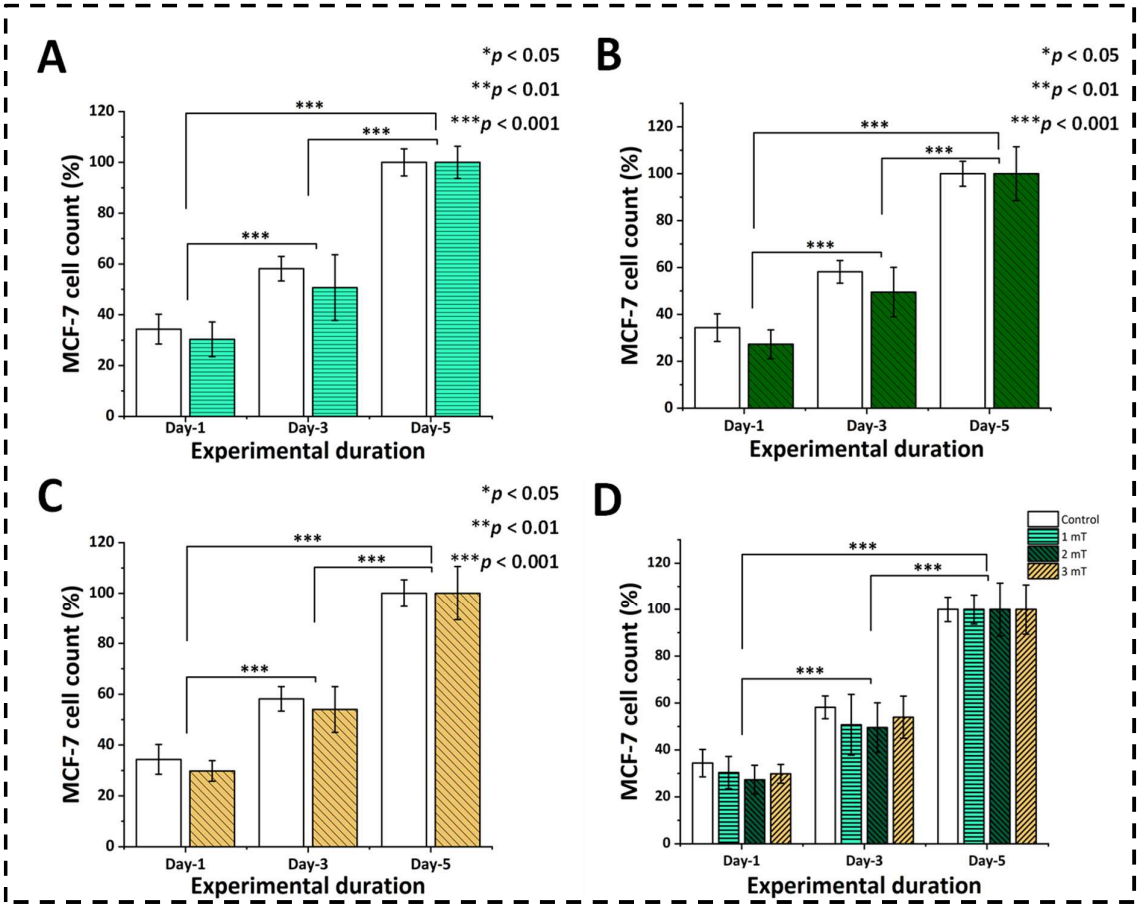

Figure 5.5 Cell count % of breast cancer (MCF-7) cells was found unaffected by the to 50 Hz ELF-PEMF (horizontally aligned) exposure. MCF-7 cells count at different MF intensities (1-3 mT, 20 min (twice) with 4 h gap) over 5 days. **(A)** Effects of 1 mT on MCF-7 cell count compared to control, **(B)** Effects of 2 mT on MCF-7 cell count compared to control, **(C)** Effects of 3 mT on MCF-7 cell count compared to control, **(D)** Comparative analysis of MF exposure on MCF-7 cells compared to control group. The initial seeding concentration was 1×10^3 cells/well, and MF exposure till the 5th day or confluency (≥ 95%). The independent exposures were performed in triplicates. "*" $p < 0.05$, "**" $p < 0.01$, "***" $p < 0.001$.

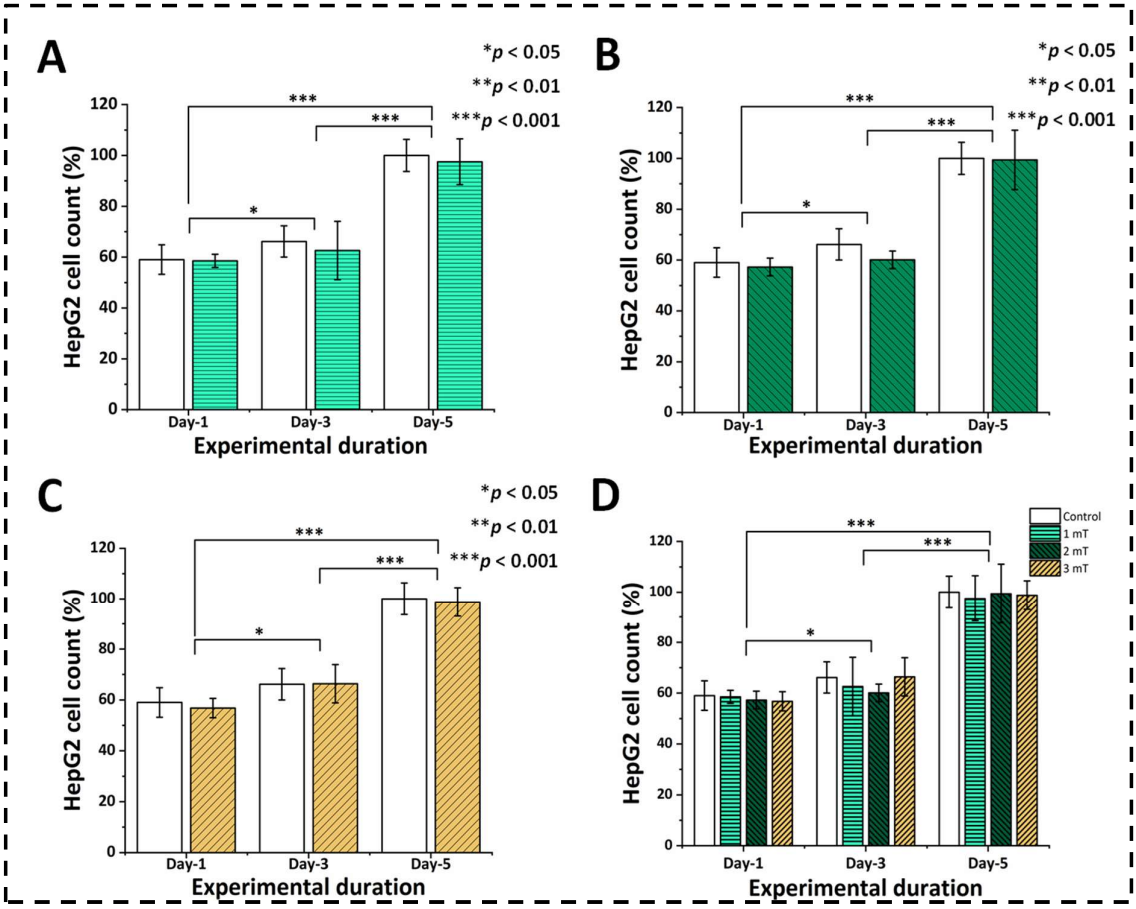

Figure 5.6 Cell count% of hepatoblastoma (HepG2) cells was unaffected by the 50 Hz ELF-PEMF exposure (horizontally aligned). HepG2 cells count at different MF intensities (1-3 mT, 20 min (twice) with 4 h gap) over 5 days. **(A)** Effects of 1 mT on HepG2 cell count compared to control, **(B)** Effects of 2 mT on HepG2 cell count compared to control, **(C)** Effects of 3 mT on HepG2 cell count compared to control, **(D)** Comparative analysis of MF exposure on HepG2 cells compared to control group. The initial seeding concentration was 1×10^3 cells/well, and MF exposure till the 5th day or confluency ($\geq$ 95%). The independent exposures were performed in triplicates. "*" $p < 0.05$, "**" $p < 0.01$, "***" $p < 0.001$.

5.4.2 Effects on cell morphologies

Fluorescence microscopy methods were used to determine the extent of changes in cell morphology induced by 50 Hz magnetic field exposure in A549 cells. Following cell exposure to 50 Hz ELF-PEMF, morphological alterations of A549 cells are depicted in figure (5.7). In comparison to the control group, cells exposed to 50 Hz ELF-PEMF displayed alterations in cellular morphology, such as a decrease in cell volume, a disruption of the actin cytoskeleton,

and a shrinking of the cell nuclei. The percentage of cell proliferation was also observed in exposed cells, as mentioned in above sections. The 50 Hz magnetic field exposure reduced the number of viable A549 cells depending on exposure intensity, frequency, and duration.

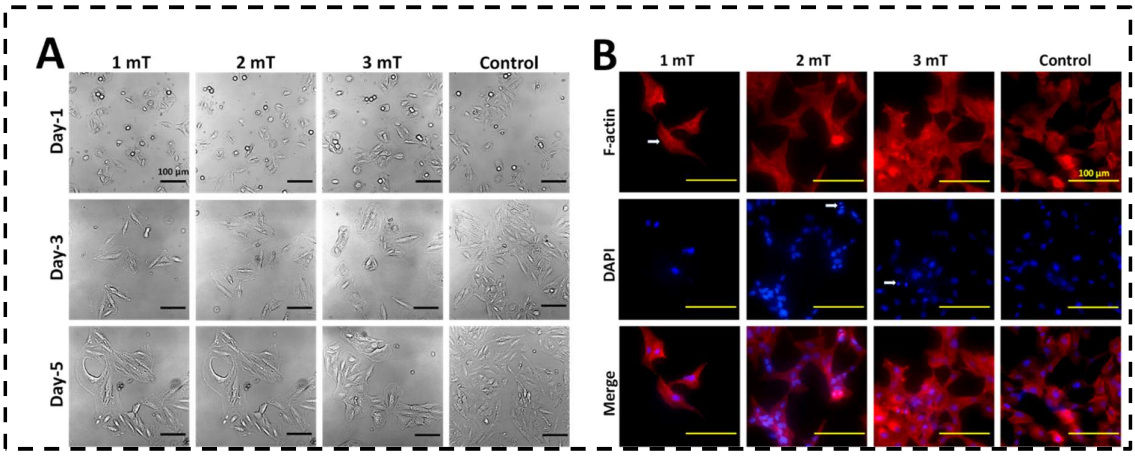

Figure 5.7 Effects of 50 Hz ELF-PEMF exposure (1-3 mT, 20 min (twice) with 4 h gap) on cell proliferation and morphology of A549 cells as observed through the analysis of microscopic images. **(A)** A representative panel of bright-field images of A549 cells stimulated by magnetic field of different strengths, **(B)** A representative panel of fluorescent images of A549 cells stimulated by magnetic field of different strengths. Scale bar: 100 µm for bright-field, fluorescent, and merged images.

We also observed the effects of magnetic field exposure on confluency of MCF-7 and HepG2 cells through microscopic image analysis, which is depicted in figures 5.8 (A-B). In comparison to the control group, exposed cells do not display any alterations cell volume and rate of proliferations.

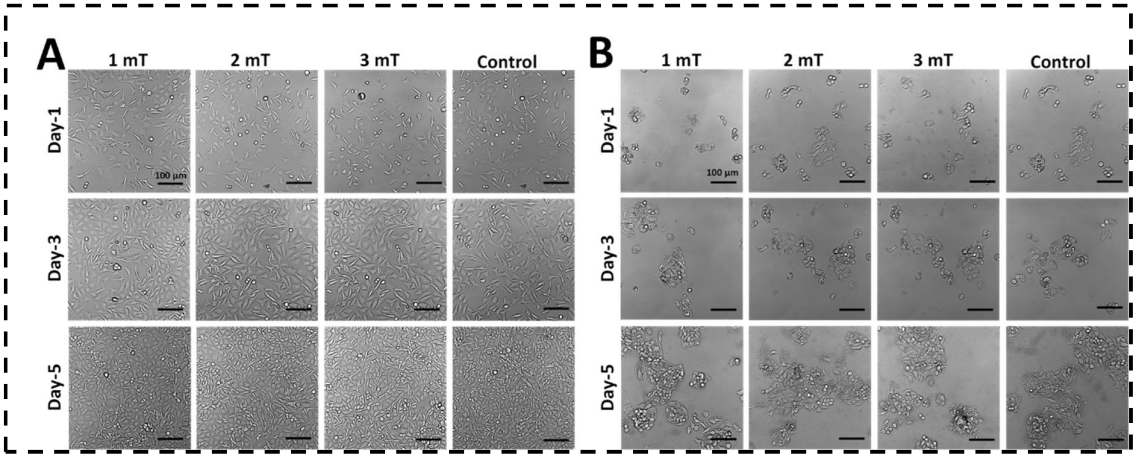

Figure 5.8 Effect 50 Hz ELF-PEMF exposure (1-3 mT, 20 min (twice) with 4 h gap) on proliferation and morphology of MCF-7 and HepG2 cells as observed through qualitative analysis of microscopic images. **(A)** A representative panel of bright-field images of MCF-7 cells stimulated by magnetic field of different strengths, **(B)** A representative panel of fluorescent images of HepG2 cells stimulated by magnetic field of different strengths. Scale bar: 100 µm for bright-field images.

5.4.3 MTT analysis

Figure 5.9 (A-D) shows the proliferation of the A549 cell cultures exposed to 50 Hz ELF-PEMF intensities (1-3 mT) relative to control. The bar plot of figures 5.9 (A-C) shows only the exposure effects of single intensities from day 1 to day 5. In contrast, figure 5.9 (D) (see below) is the comparative interpretation through statistical analysis. All values of A.C. M.F. in the upcoming text and figures are peak values around the center of the coils. For magnetic field exposure (1 mT), cell proliferation % on day 1 is not much affected. Still, from day 3 to day 5, it is significantly reduced compared to the control group, as shown in figure 5.9 (A). Similarly, 2 mT and 3 mT also caused a significant reduction in cell proliferation % after day 3 to day 5 compared to respective control groups, as shown in figures 5.9 (B-C). The cellular viability of A549 cells over different magnetic field intensities is included in table 5.2.

Since we were interested in inhibiting cancer cell proliferation, we decided to determine the exposure effects on the other two cancer cell lines (Figures 5.10-5.11). We observed that A549

was responsive to all values of 50 Hz ELF-PEMF with a maximum decrease in proliferation of 24 % compared to control ($p < 0.001$), while the MCF-7 and HepG2 were not responsive. No difference existed between the exposure intensities, frequency, duration, and experimental conditions. The cellular viabilities of MCF-7 and HepG2 cells over different magnetic field intensities are included in table 5.3 & 5.4. No change in cell proliferation % was observed between exposed and controls in any of the experiments.

Table 5.2 Effect of 50 Hz ELF-PEMF exposure (1-3 mT) on A549 cells assessed through the MTT assay.

Magnetic field exposure for 5 days or till confluency (≥ 95%) in the control group	**Cellular viability (%)**		
	Day-1	**Day-3**	**Day-5**
1 mT	47.49 ± 3.84	75.10 ± 4.72	76.52 ± 7.11
2 mT	44.74 ± 1.17	72.90 ± 6.21	84.49 ± 10.98
3 mT	49.43 ± 3.37	73 ± 11.19	97.56 ±7.78

Table 5.3 Effect of 50 ELF-PEMF exposure (1-3 mT) on MCF-7 cells assessed through the MTT assay.

Magnetic field exposure for 5 days or till confluency (≥ 95%) in the control group	**Cellular viability**		
	Day-1	**Day-3**	**Day-5**
1 mT	31.44 ± 0.73	49.57 ± 2.44	101.90 ± 1.16
2 mT	31.54 ± 1.46	49.22 ± 2.94	97.29 ± 1.50
3 mT	30.93 ± 1.98	49.01 ± 1.58	101.3 ± 2.35

Table 5.4 Effect 50 Hz ELF-PEMF exposure (1-3 mT) on HepG2 cells assessed through the MTT assay

Magnetic field exposure for 5 days or till confluency (≥ 95%) in the control group	Cellular viability (%)		
	Day-1	Day-3	Day-5
1 mT	76.51 ± 9.9	78.80 ± 14.55	97.97 ± 12.33
2 mT	76.10 ± 5.45	77.41 ± 10.35	99.75 ± 13.71
3 mT	75.28 ± 6.93	78.80 ± 10.42	101.41 ± 10.86

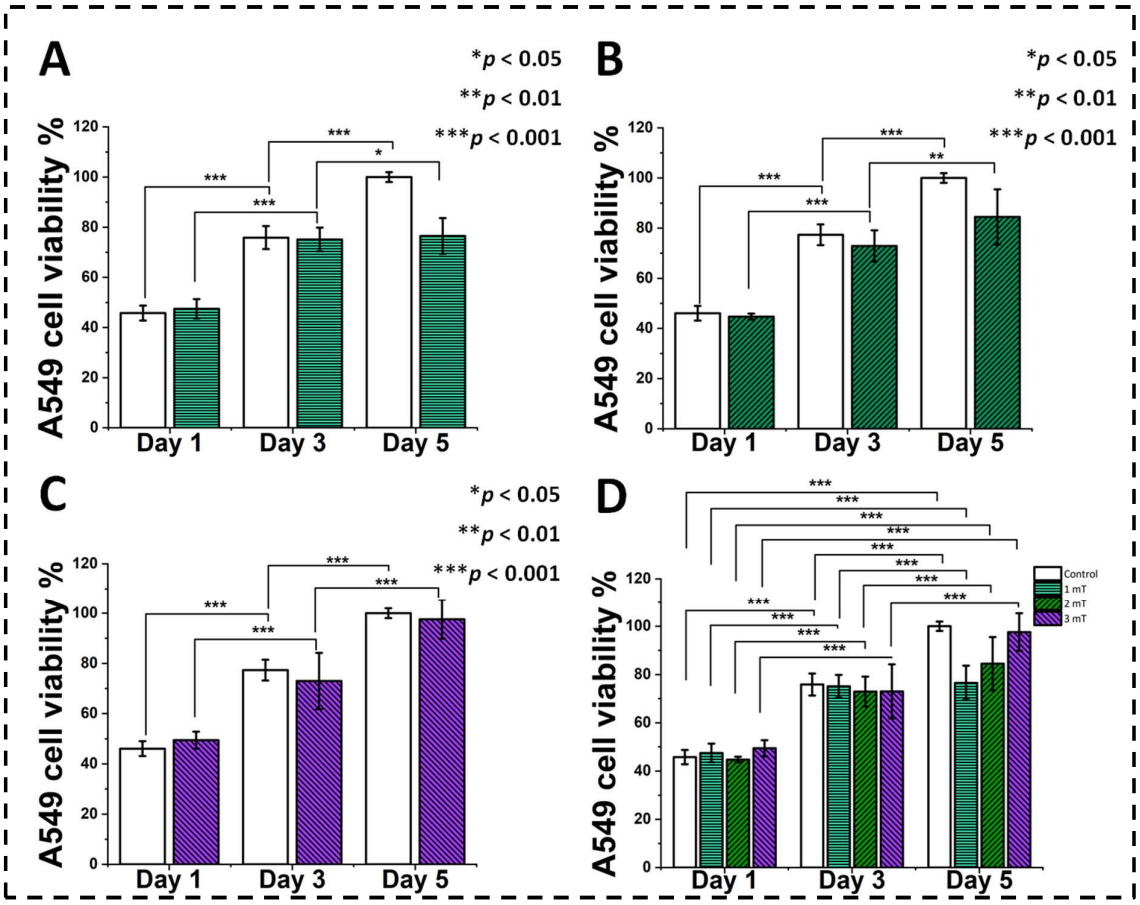

Figure 5.9 Effects of 50 Hz ELF-PEMF exposure (1-3 mT) on cell viabilities of A549 cells compared with control. Cells were incubated for 5 days or confluency (≥ 95%), and magnetic field was applied daily for the indicated duration. **(A)** A549 cells exposed with 1 mT compared with control, **(B)** A549 cells exposed with 2 mT compared with control, **(C)** A549 cells exposed

with 3 mT compared with control, **(D)** Comparative analysis of magnetic field exposure on A549 cells. The independent exposures were performed in triplicates. "*" $p < 0.05$, "**" $p < 0.01$, "***" $p < 0.001$.

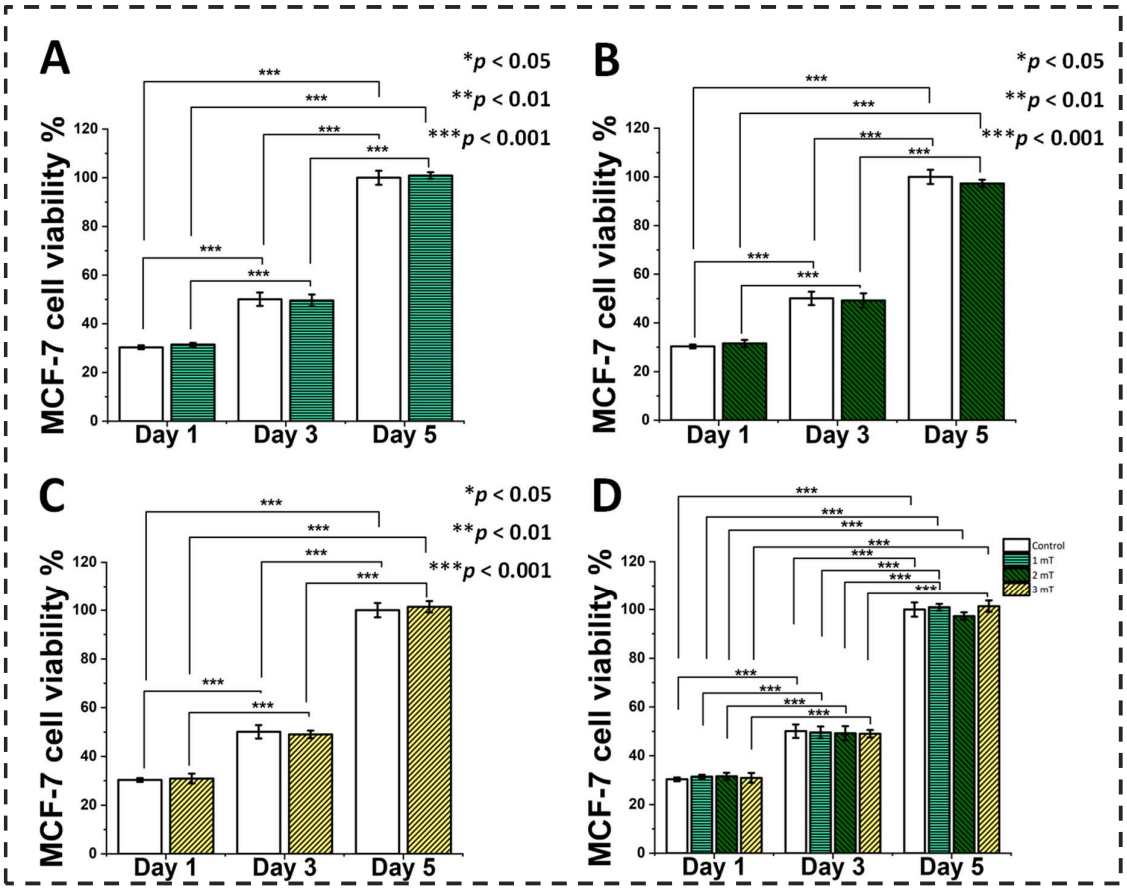

Figure 5.10 Effects of 50 Hz ELF-PEMF exposure (1-3 mT) on cell viabilities of MCF-7 cells compared with control. Cells were incubated for 5 days or confluency (≥ 95%), and magnetic field was applied daily for the indicated duration. **(A)** MCF-7 cells exposed with 1 mT compared with control, **(B)** MCF-7 cells exposed with 2 mT compared with control, **(C)** MCF-7 cells exposed with 3 mT compared with control, **(D)** Comparative analysis of magnetic field exposure on MCF-7 cells. The independent exposures were performed in triplicates. "*" $p < 0.05$, "**" $p < 0.01$, "***" $p < 0.001$.

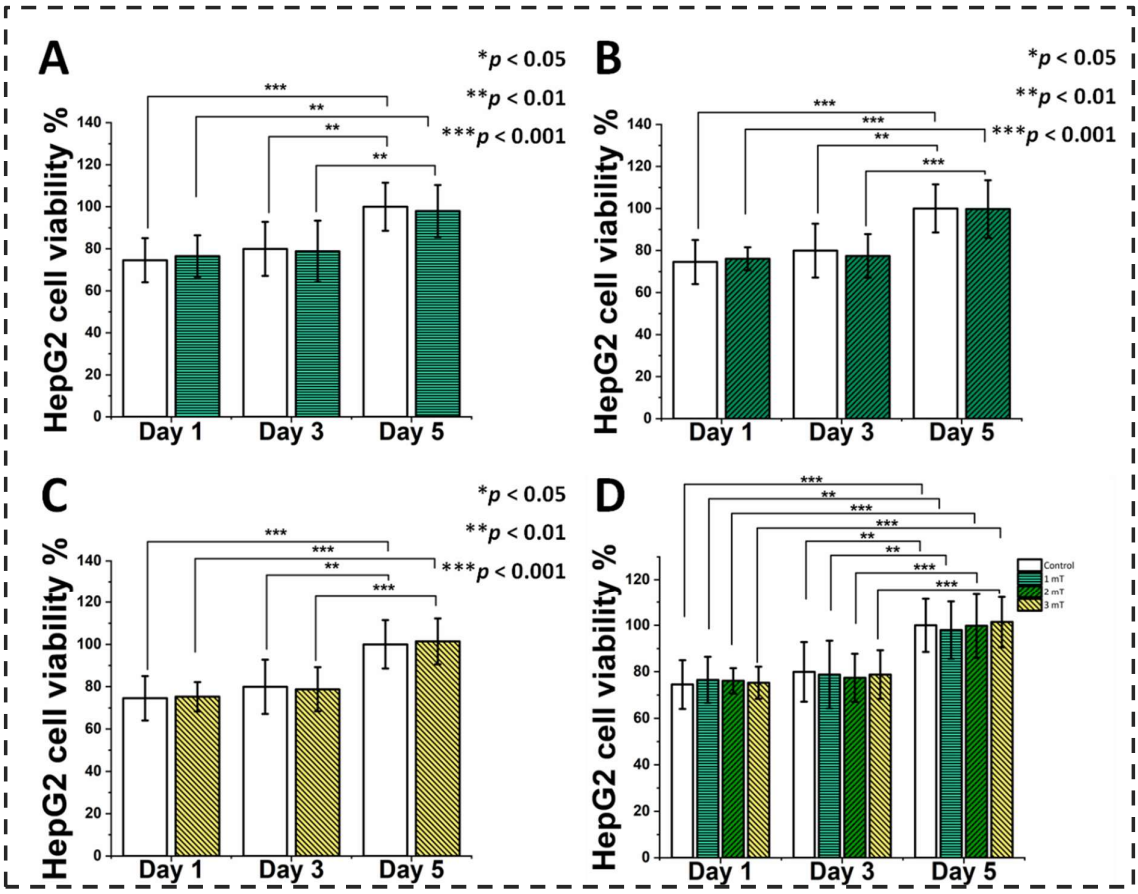

Figure 5.11 Effects of 50 Hz ELF-PEMF exposure (1-3 mT) on cell viabilities of HepG2 cells compared with control. Cells were incubated for 5 days or confluency (≥ 95%), and magnetic field was applied daily for the indicated duration. **(A)** HepG2 cells exposed with 1 mT compared with control, **(B)** HepG2 cells exposed with 2 mT compared with control, **(C)** HepG2 cells exposed with 3 mT compared with control, **(D)** Comparative analysis of magnetic field exposure on HepG2 cells. The independent exposures were performed in triplicates. "*" $p < 0.05$, "**" $p < 0.01$, "***" $p < 0.001$.

Table 5.5 Effects of 50 Hz magnetic field exposure on cell morphology of different cancer cell lines.

Cell lines	**Observed effects**			**Conclusion**
	1 mT	**2 mT**	**3 mT**	
Cancerous cell				

Lung adenocarcinoma (A549)	Significant changes in f-actin distribution and shrinkage of cell nuclei are observed.	Depending on exposure parameters, magnetic field exposure induces cell death and shrinkage in A549 cells.
Breast cancer (MCF-7)	No changes in cell proliferation and morphology.	MCF-7 cells are insensitive to magnetic field exposure under present experimental conditions.
Hepatocellular carcinoma (HepG2)	No changes in cell proliferation and morphology were observed.	HepG2 cells are insensitive to magnetic field exposure under present experimental conditions.
Non-cancerous cell		
Glial cells (C6)	No sign of cell fragmentation or change in morphology is observed.	No harmful effects on C6 cells.
Mouse fibroblast (RFP-L929)	No sign of cell fragmentation or change in morphology is observed.	No harmful effects on RFP-L929.

5.5 Discussion:

In present scenario, the electromagnetic field exposure has increased multifold in occupational and household environment (Kaune et al., 2000; Protection, 2007; Sciences and Health, 2002). The electromagnetic field utilized in the household appliances are primarily in the range of ≤ 100 kHz, which also includes power frequency (50/60 Hz) (Protection, 2020, 2010; Protection (ICNIRP)1, 2020). Previous studies proposed that magnetic field exposure (< 20 mT) with duration (> 1 h/day) can affect biochemical parameters and enzymes (Buckner et al., 2018; Ibrahim et al., 2018; Jeong et al., 2014; Kulkarni and Gandhare, 2015; Pohling et al., 2023). Alternatively, we observed the 50 Hz ELF-PEMF (1-3 mT) exposure with duration (20 min (twice) with 4 h gap) effects on behavioral parameters (spontaneous alternation, anxiety,

locomotor activity), biochemical parameters (AST, ALT, TBIL, serum creatinine & Ck-MB) and cell proliferation (RFP-L929, C6) under *in vivo* and *in vitro* conditions, respectively (Tekam et al., 2023a). The results indicated no significant effects on above mentioned parameters, which motivated us to observe the magnetic field effects on different cancer cell lines. According to previous studies 50 Hz ELF-PEMF exposure causing inhibition or stimulation of cell proliferation primarily depends on cell type (cancerous/non-cancerous) and exposure conditions (Olsson et al., 2001; Verheyen et al., 2003). The 50 Hz is naturally a parameter in power line fields to observe carcinogenic, antiproliferative effects. Whether a natural reaction to the A.C. (50 Hz) fields have an amplitude window is still poorly understood. However, based on the currently accessible electromagneto-biology research, the results may vary based on the experimental conditions. The selection of intensities of A.C. magnetic fields and exposure duration (< 1 h/day) can be essential factors in finding a significant biological response in cancer cells when looking for a potentially therapeutic application. Hence, ELF-PEMF intensities (1-3 mT) and duration (20 min(twice) with 4 h gap) is selected to avoid any chances of non-thermal consequences on cells which is in agreement of previous literatures (Cifra et al., 2011; Marino and Becker, 1977; Zadeh-Haghighi and Simon, 2022).

The antiproliferative effects of 50 Hz ELF-PEMF exposure can be explained according to some fundamental mechanisms: cell cycle arrest, rippling and nanopore formation, p53 protein, and activation of P53-miR-34a-E2F1/E2F3 pathways (Adrain and Martin, 2001; Ashdown et al., 2020; Simon et al., 2000; Vigneswara and Ahmed, 2020). The cancer cell inhibition through a non-invasive approach is particularly interesting since it may represent comparatively safe and effective methodologies in cancer treatment. Hence, the present work aimed to demonstrate the feasibility of using the monoaxial Helmholtz coil method to screen A549, MCF-7, and HepG2 cells for 50 Hz ELF-PEMF (1-3 mT) exposures with duration (< 1 h/day). We observed that the A549 cells demonstrated a significant reduction in cell count% and altered cell

morphologies, as depicted in figure (5.4) and figure (5.7), respectively. Moreover, MTT analysis also supported the antiproliferative impact of 50 Hz ELF-PEMF exposure on A549 cells, as shown in figure (5.9). However, MCF-7 and HepG2 cells were unaffected under current experimental conditions, suggesting that each cell type may respond differently to the ELF-PEMF, as shown in figures (5.5-5.6) and figures (5.10-5.11). Previous studies mentioned DNA strand breaks and rippling in cell membranes upon exposure to the ELF-MF (Ashdown et al., 2020; Focke et al., 2010). The variation in MF sensitivity draws attention to the potential impacts of a 50 Hz magnetic field on cancer cells' mitochondrial function. Destefanis et al. observed that an MF (12 μT (rms), 50 Hz, 7 days) inhibited cell proliferation and altered the mitochondrial protein profile of different cancer cell lines (Destefanis et al., 2015). Simko et al. also suggested that the variability in the redox status of exposed cell lines could explain the effects under identical conditions (Simko, 2007). Numerous scientific studies have validated that different 50 Hz MF exposures can elicit different responses on different cell lines (Alkis et al., 2022; Destefanis et al., 2015; Filipovic et al., 2014; Spyridopoulou et al., 2018). Based on the wide range of existing literature, we can postulate that different cancer cells exhibit a wide range of responses: either a significant reduction in cell proliferation or no effects, solely dependent on experimental conditions.

It should be noted that, despite the growing body of research on the topic, no solid biophysical reasoning has yet been provided for precisely defining the exposure parameters that should be investigated as potentially therapeutic. Still, we have determined the biologically effective and safe 50 Hz ELF-PEMF range and exposure duration for future biomedical applications, aligning with previous studies as illustrated in table 5.5. After considering all of the previously mentioned factors, we can only conclude that the topic is still very complex and that a desirable, if not necessary, course of action for determining the biophysical mechanisms underlying the

interaction of ELF-MF with biological tissues would be to carefully screen through the various exposure parameters (intensity, frequency, duration, etc.).

5.6 Conclusion

We have shown for the first time that a 50 Hz ELF-PEMF exposure (1-3 mT) (horizontal) with duration (< 1 h/day) can directly affect biological responses at the cellular level. Furthermore, we also observed that weak ELF-MF, inhibited the proliferation of A549 cancer cells depending on their strength, frequency, and duration. Our results also support earlier studies by showing that different cell lines can respond differently to exposure to the same magnetic field and that the same cell line can respond differently to fields with varying intensities. The present Helmholtz coil system constitutes a novel method of screening in the requirement for effective 50 Hz magnetic field parameters to influence cancer cell proliferation.

5.7 References:

Adrain, C., Martin, S.J., 2001. The mitochondrial apoptosome: a killer unleashed by the cytochrome seas. Trends Biochem. Sci. 26, 390–397. https://doi.org/10.1016/s0968-0004(01)01844-8

Ahlbom, A., Bridges, J., De Seze, R., Hillert, L., Juutilainen, J., Mattsson, M.-O., Neubauer, G., Schüz, J., Simko, M., Bromen, K., 2008. Possible effects of electromagnetic fields (EMF) on human health–opinion of the scientific committee on emerging and newly identified health risks (SCENIHR). Toxicology 246, 248–50.

Alkis, M.E., Akdag, M.Z., Kandemir, S.I., 2022. Influence of extremely low-frequency magnetic field on chemotherapy and electrochemotherapy efficacy in human Caco-2 colon cancer cells. Electromagn. Biol. Med. 41, 177–183.

Ashdown, C.P., Johns, S.C., Aminov, E., Unanian, M., Connacher, W., Friend, J., Fuster, M.M., 2020. Pulsed Low-Frequency Magnetic Fields Induce Tumor Membrane

Disruption and Altered Cell Viability. Biophys. J. 118, 1552–1563. https://doi.org/10.1016/j.bpj.2020.02.013

Barati, M., Darvishi, B., Javidi, M.A., Mohammadian, A., Shariatpanahi, S.P., Eisavand, M.R., Madjid Ansari, A., 2021. Cellular stress response to extremely low-frequency electromagnetic fields (ELF-EMF): An explanation for controversial effects of ELF-EMF on apoptosis. Cell Prolif. 54, e13154. https://doi.org/10.1111/cpr.13154

Belyaev, I., Dean, A., Eger, H., Hubmann, G., Jandrisovits, R., Kern, M., Kundi, M., Moshammer, H., Lercher, P., Müller, K., Oberfeld, G., Ohnsorge, P., Pelzmann, P., Scheingraber, C., Thill, R., 2016. EUROPAEM EMF Guideline 2016 for the prevention, diagnosis and treatment of EMF-related health problems and illnesses. Rev. Environ. Health 31, 363–397. https://doi.org/10.1515/reveh-2016-0011

Buckner, C.A., Buckner, A.L., Koren, S.A., Persinger, M.A., Lafrenie, R.M., 2018. Exposure to a specific time-varying electromagnetic field inhibits cell proliferation via cAMP and ERK signaling in cancer cells. Bioelectromagnetics 39, 217–230. https://doi.org/10.1002/bem.22096

Cifra, M., Fields, J.Z., Farhadi, A., 2011. Electromagnetic cellular interactions. Prog. Biophys. Mol. Biol., Muscle Excitation-Contraction Coupling: Elements and Integration 105, 223–246. https://doi.org/10.1016/j.pbiomolbio.2010.07.003

Crocetti, S., Beyer, C., Schade, G., Egli, M., Fröhlich, J., Franco-Obregón, A., 2013. Low intensity and frequency pulsed electromagnetic fields selectively impair breast cancer cell viability. PloS One 8, e72944.

Destefanis, M., Viano, M., Leo, C., Gervino, G., Ponzetto, A., Silvagno, F., 2015. Extremely low frequency electromagnetic fields affect proliferation and mitochondrial activity of human cancer cell lines. Int. J. Radiat. Biol. 91, 964–972. https://doi.org/10.3109/09553002.2015.1101648

Dj, P., N, M., A, K., Al, P., Lh, M., 2000. A mechanism for action of oscillating electric fields on cells. Biochem. Biophys. Res. Commun. 272. https://doi.org/10.1006/bbrc.2000.2746

Dubey, A.K., Lavanya, L., Sadananda, D., Gouthami, K., Elfansu, K., Singh, A., 2021. Inferences of Carbon Dioxide in Present-Day Cell Culture Systems: An Unacknowledged Problem and Perspectives. Austin Ther 6, 26420.

Filipovic, N., Djukic, T., Radovic, M., Cvetkovic, D., Curcic, M., Markovic, S., Peulic, A., Jeremic, B., 2014. Electromagnetic field investigation on different cancer cell lines. Cancer Cell Int. 14, 1–10.

Focke, F., Schuermann, D., Kuster, N., Schär, P., 2010. DNA fragmentation in human fibroblasts under extremely low frequency electromagnetic field exposure. Mutat. Res. Mol. Mech. Mutagen. 683, 74–83.

Foster, J.R., 1997. The role of cell proliferation in chemically induced carcinogenesis. J. Comp. Pathol. 116, 113–144. https://doi.org/10.1016/S0021-9975(97)80071-0

Funk, R.H.W., Monsees, T., Özkucur, N., 2009. Electromagnetic effects – From cell biology to medicine. Prog. Histochem. Cytochem. 43, 177–264. https://doi.org/10.1016/j.proghi.2008.07.001

Ghodbane, S., Lahbib, A., Sakly, M., Abdelmelek, H., 2013. Bioeffects of static magnetic fields: oxidative stress, genotoxic effects, and cancer studies. BioMed Res. Int. 2013.

Hall, E.H., Schoenbach, K.H., Beebe, S.J., 2005. Nanosecond pulsed electric fields (nsPEF) induce direct electric field effects and biological effects on human colon carcinoma cells. DNA Cell Biol. 24, 283–291.

Ibrahim, N., Hajalan, S., Wajih, A., Khudhair, N., Khalid, A., Thaker, A.A., 2018. Study the effect of electromagnetic field on some physiological and histological characteristics on the liver of mice. Asian Jr Microbiol Biotech Env Sc 20, S41–S46.

Jablonská, E., Horkavcová, D., Rohanová, D., S. Brauer, D., 2020. A review of in vitro cell culture testing methods for bioactive glasses and other biomaterials for hard tissue regeneration. J. Mater. Chem. B 8, 10941–10953. https://doi.org/10.1039/D0TB01493A

Jeong, H., Sung, J., Oh, S., Jeong, S., Koh, E.K., Hong, S., Yoon, M., 2014. Inhibition of brain tumor cell proliferation by alternating electric fields. Appl. Phys. Lett. 105, 203703. https://doi.org/10.1063/1.4902112

Kaune, W. t., Miller, M. c., Linet, M. s., Hatch, E. e., Kleinerman, R. a., Wacholder, S., Mohr, A. h., Tarone, R. e., Haines, C., 2000. Children's exposure to magnetic fields produced by U.S. television sets used for viewing programs and playing video games. Bioelectromagnetics 21, 214–227. https://doi.org/10.1002/(SICI)1521-186X(200004)21:3<214::AID-BEM8>3.0.CO;2-Y

Kulkarni, G., Gandhare, W., 2015. Effect of extremely low frequency electric field on liver, kidney, and lipids of Wistar rats. Int J Med Sci Public Heal 4, 1755.

Lichtman, J.W., Conchello, J.-A., 2005. Fluorescence microscopy. Nat. Methods 2, 910–919. https://doi.org/10.1038/nmeth817

Mahna, A., Firoozabadi, S.M.P., Shankayi, Z., 2014. The effect of ELF magnetic field on tumor growth after electrochemotherapy. J. Membr. Biol. 247, 9–15.

Marino, A.A., Becker, R.O., 1977. Biological effects of extremely low frequency electric and magnetic fields: a review. Physiol Chem Phys 9, 131–147.

Mattiuzzi, C., Lippi, G., 2019. Current Cancer Epidemiology. J. Epidemiol. Glob. Health 9, 217–222. https://doi.org/10.2991/jegh.k.191008.001

Olsson, G., Belyaev, I.Y., Helleday, T., Harms-Ringdahl, M., 2001. ELF magnetic field affects proliferation of SPD8/V79 Chinese hamster cells but does not interact with

intrachromosomal recombination. Mutat. Res. Toxicol. Environ. Mutagen. 493, 55–66. https://doi.org/10.1016/S1383-5718(01)00158-9

Panagopoulos, D.J., Karabarbounis, A., Margaritis, L.H., 2002. Mechanism for action of electromagnetic fields on cells. Biochem. Biophys. Res. Commun. 298, 95–102. https://doi.org/10.1016/S0006-291X(02)02393-8

Pohling, C., Nguyen, H., Chang, E., Schubert, K.E., Nie, Y., Bashkirov, V., Yamamoto, V., Zeng, Y., Stupp, R., Schulte, R.W., Patel, C.B., 2023. Current status of the preclinical evaluation of alternating electric fields as a form of cancer therapy. Bioelectrochemistry 149, 108287. https://doi.org/10.1016/j.bioelechem.2022.108287

Pollard, T.D., 2016. Actin and Actin-Binding Proteins. Cold Spring Harb. Perspect. Biol. 8, a018226. https://doi.org/10.1101/cshperspect.a018226

Protection, I.C. on N.-I.R., 2020. Guidelines for limiting exposure to electromagnetic fields (100 kHz to 300 GHz). Health Phys. 118, 483–524.

Protection, I.C. on N.-I.R., 2010. Guidelines for limiting exposure to time-varying electric and magnetic fields (1 Hz to 100 kHz). Health Phys. 99, 818–836.

Protection (ICNIRP)1, I.C. on N.-I.R., 2020. Guidelines for Limiting Exposure to Electromagnetic Fields (100 kHz to 300 GHz). Health Phys. 118, 483. https://doi.org/10.1097/HP.0000000000001210

Protection, N.-I.R., 2007. Extremely Low Frequency fields. World Health Organ.

Radeva, M., Berg, H., 2004. Differences in lethality between cancer cells and human lymphocytes caused by LF-electromagnetic fields. Bioelectromagn. J. Bioelectromagn. Soc. Soc. Phys. Regul. Biol. Med. Eur. Bioelectromagn. Assoc. 25, 503–507.

Sciences, N.I. of E.H., Health, N.I. of, 2002. EMF Electric and Magnetic Fields Associated with the Use of Electric Power. Quest. Answ. Res. Triangle Park NC NIEHSDOE EMF RAPID Program.

Simko, M., 2007. Cell Type Specific Redox Status is Responsible for Diverse Electromagnetic Field Effects. Curr. Med. Chem. 14, 1141–1152. https://doi.org/10.2174/092986707780362835

Simon, H.U., Haj-Yehia, A., Levi-Schaffer, F., 2000. Role of reactive oxygen species (ROS) in apoptosis induction. Apoptosis Int. J. Program. Cell Death 5, 415–418. https://doi.org/10.1023/a:1009616228304

Spyridopoulou, K., Makridis, A., Maniotis, N., Karypidou, N., Myrovali, E., Samaras, T., Angelakeris, M., Chlichlia, K., Kalogirou, O., 2018. Effect of low frequency magnetic fields on the growth of MNP-treated HT29 colon cancer cells. Nanotechnology 29, 175101.

Stockert, J.C., Horobin, R.W., Colombo, L.L., Blázquez-Castro, A., 2018. Tetrazolium salts and formazan products in Cell Biology: Viability assessment, fluorescence imaging, and labeling perspectives. Acta Histochem. 120, 159–167. https://doi.org/10.1016/j.acthis.2018.02.005

Tekam, C.K.S., Majumdar, S., Kumari, P., Prajapati, S.K., Sahi, A.K., Shinde, S., Singh, R., Samaiya, P.K., Patnaik, R., Krishnamurthy, S., Mahto, S.K., 2023a. Effects of ELF-PEMF exposure on spontaneous alternation, anxiety, motor co-ordination and locomotor activity of adult wistar rats and viability of C6 (Glial) cells in culture. Toxicology 485, 153409. https://doi.org/10.1016/j.tox.2022.153409

Tekam, C.K.S., Sahi, A.K., Shinde, S., Kumari, P., Mahto, S.K., 2023b. Design and Development of Extremely Low-Frequency Pulsed Electro-magnetotherapy Chamber for In Vivo and In Vitro Studies. Eur. Chem. Bull. 12, 9559–9578. https://doi: 10.48047/ecb/2023.12.si4.858

Thrivikraman, G., Boda, S.K., Basu, B., 2018. Unraveling the mechanistic effects of electric field stimulation towards directing stem cell fate and function: A tissue engineering

perspective. Biomaterials 150, 60–86. https://doi.org/10.1016/j.biomaterials.2017.10.003

Uckun, F.M., Kurosaki, T., Jin, J., Jun, X., Morgan, A., Takata, M., Bolen, J., Luben, R., 1995. Exposure of B-lineage Lymphoid Cells to Low Energy Electromagnetic Fields Stimulates Lyn Kinase (*). J. Biol. Chem. 270, 27666–27670. https://doi.org/10.1074/jbc.270.46.27666

Verheyen, G. r., Pauwels, G., Verschaeve, L., Schoeters, G., 2003. Effect of coexposure to 50 Hz magnetic fields and an aneugen on human lymphocytes, determined by the cytokinesis block micronucleus assay. Bioelectromagnetics 24, 160–164. https://doi.org/10.1002/bem.10100

Vigneswara, V., Ahmed, Z., 2020. The Role of Caspase-2 in Regulating Cell Fate. Cells 9, 1259. https://doi.org/10.3390/cells9051259

Zadeh-Haghighi, H., Simon, C., 2022. Magnetic field effects in biology from the perspective of the radical pair mechanism. J. R. Soc. Interface 19, 20220325. https://doi.org/10.1098/rsif.2022.0325